Observation of a possible tetrahedratic phase in a bent-core liquid crystal

D. Wiant, K. Neupane, S. Sharma, J. T. Gleeson, and S. Sprunt
Department of Physics Kent State University, Kent, Ohio 44242, USA

A. Jákli
Chemical Physics Interdisciplinary Program and Liquid Crystal Institute, Kent State University, Kent, Ohio 44242, USA

N. Pradhan and G. Iannacchione
Department of Physics, Worcester Polytechnic Institute, Worcester, Massachusetts 01609, USA

(Received 9 November 2006; revised manuscript received 13 March 2008; published 2 June 2008)

An experimental study of the heat capacity, mass density, magnetic-field-induced optical birefringence, linewidth and intensity of scattered light, and the viscosities associated with nematic order parameter fluctuations and fluid flow has been performed on an achiral bent-core liquid crystal above its clearing point temperature. The measurements reveal a transition between two optically isotropic phases that is consistent with recent theoretical predictions of a "tetrahedratic" form of orientational order.

DOI: 10.1103/PhysRevE.77.061701 PACS number(s): 61.30.Eb, 61.30.Cz, 78.35.+c

Over the past decade, bent-core liquid crystals have generated much interest due to their spontaneously chiral and/or polar smectic phases [1–5], which have no analog in classic calamitic (rod-shaped) liquid crystal systems. More recently, the nematic phases of bent-core materials have attracted attention based on reports of biaxiality [6–8] and giant flexoelectric effects [9]. In addition, several exotic bent-core phases, including spontaneously chiral and macroscopically polar nematic phases as well as an optically isotropic but orientationally ordered "tetrahedratic" phase [10], have been theoretically predicted [11,12] as possible consequences of bent-shaped mesogens. So far, none of these possibilities has been experimentally confirmed. Interestingly, however, previous dynamic light scattering [13], magnetic-field-induced birefringence [13], and NMR measurements [14] on bent-core liquid crystals do reveal unusual properties associated with the isotropic phase and the isotropic-nematic (*I-N*) transition. For a particularly well-studied compound, 4-chloro-1,3-phenylenebis[4-(4-9-decenyloxy) benzoyloxy benzoate] (ClPbis10BB) [15], important parameters—ranging from the magnitude of the leading Landau coefficient in the standard Landau–de Gennes (LdG) free energy used to describe the transition to the viscosity for nematic order parameter fluctuations [13]—differ markedly from the corresponding values observed in calamitics at comparable temperature increments ($T-T_{cp}$) above the clearing point temperature (T_{cp}).

In this paper, we present ac calorimetry, mass density, magnetic birefringence, light scattering, and viscosity measurements on ClPbis10BB that reveal a transition between distinct optically isotropic phases occurring above T_{cp} together with an interesting combination of expected and unusual pretransitional behavior observed on approaching the nematic phase. We argue that our results can be understood in the framework of a form of orientational order characterized by a symmetric, traceless, third-rank tensor order parameter τ_{ijk} [10–12]—and designated tetrahedratic order—which does not carry with it the optical anisotropy characteristic of the second-rank tensor order parameter Q_{ij} that conventionally describes the nematic phase. The tetrahedratic or τ phase is envisioned as being made up of nanoscopic molecular complexes that possess a tetrahedral symmetry; it is predicted to occur between a true (or fully) isotropic phase and a nematic-tetrahedratic phase (which would develop through a uniaxial distortion of the tetrahedral complexes). Theoretical arguments [11,12] suggest that bent-core mesogens are particularly favorable for formation of a τ phase. Our present study provides significant evidence for this novel form of orientational order.

To establish the existence of two distinct optically isotropic phases in ClPbis10BB above the *N* phase, we performed high-resolution ac calorimetry in the vicinity of the clearing point. In this technique, a heating power $\mathcal{P}=\mathcal{P}_0(1+\cos\omega t)$ (where $\mathcal{P}_0=0.075$ mW, $\omega=2\pi\times0.030$ s^{-1}) is delivered to the sample, and the magnitude (T_ω) and phase of the sample temperature oscillations are measured using a calibrated resistance thermometer, precision constant current source, and lock-in amplifier. T_ω was typically 7 mK. Figure 1 (top panel) shows the excess specific heat (Δc_P) of the liquid crystal sample, which is calculated from the relation $C_P=\mathcal{P}_0/\omega T_\omega$, minus the empty cell background, and then divided by the sample mass *m*. An additional quantity c_P'', associated with transitional latent heat and calculated using the amplitude of the out-of-phase component of the temperature [16], is displayed in the bottom panel. As a function of temperature, the latter reveals two well-separated peaks, and clearly establishes the presence of a pair of weakly first-order transitions, which are observed in both heating and cooling. By recording the depolarized light transmission through a thin sample, we confirmed that only one of the latent heat peaks (the one at lower temperature corresponding to T_{cp}) is associated with development of optical anisotropy. Thus, the higher-temperature peak corresponds to an isotropic-isotropic transition at a temperature we designate T_x.

We also probed the temperature dependence of the mass density of ClPbis10BB by capillary dilatometry [13,17]—i.e., by observing and recording through an optical microscope the motion of the air-liquid crystal meniscus for samples contained in an open-ended capillary. The accuracy

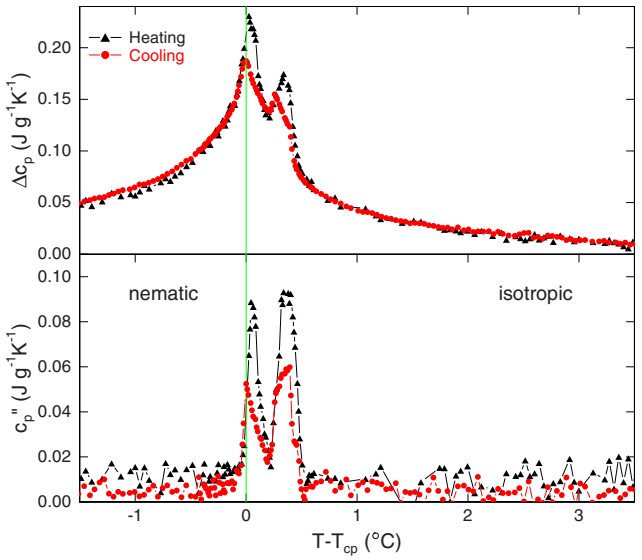

FIG. 1. (Color online) In- and out-of-phase components of the specific heat of ClPbis10BB measured by ac calorimetry. The lower-temperature peak corresponds to the optical clearing point (T_{cp}=76.9 °C); the higher peak reveals an optically isotropic-isotropic (I_1-I_2) transition at a temperature T_x=77.3 °C.

of our apparatus was established by reproducing literature values of both the density change at the nematic-isotropic transition in a conventional calamitic compound (the cyanobiphenyl 5CB) and the value of the thermal expansion coefficient of tetradecane. Figure 2 displays the incremental change in reduced mass density ($\Delta\rho/\rho$) of ClPbis10BB, following each step ΔT in temperature, while heating from the nematic phase. Since the steps ΔT are all the same, the data are proportional to the volume thermal expansion coefficient α_V. At and above the clearing point, two distinct peaks are observed in Fig. 2 at temperatures basically consistent with (though at a somewhat larger spacing than) the heat capacity

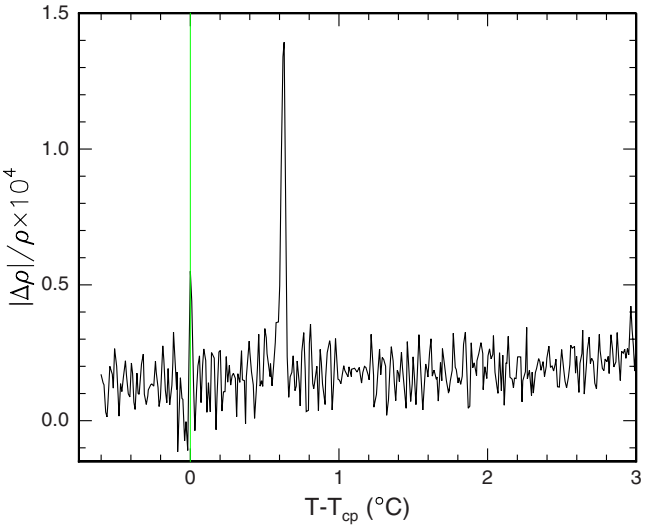

FIG. 2. (Color online) Measured change in mass density of ClPbis10BB on heating through the clearing point. The two peaks correspond to the N-I_2 and I_2-I_1 transitions detected in the heat capacity data (Fig. 1).

peaks in Fig. 1. (The difference in spacing $T_x - T_{cp}$ likely reflects the combined effects of a higher rate of change of temperature used in the density measurement, a different thermometer and liquid crystal sample, and possibly the difference in sample geometry—e.g., the use of a thin capillary in the density study.) Overall, the density data fully support the presence of distinct optically isotropic phases above the nematic phase in ClPbis10BB. Henceforth we shall refer to the lower-temperature optically isotropic phase as I_2 and the higher-temperature isotropic phase as I_1, with the observed transition sequence on cooling denoted as $I_1 \xrightarrow[T_x]{} I_2 \xrightarrow[T_{cp}]{} \mathrm{N}$.

To elucidate the nature of the I_1 and I_2 phases, we carried out magnetic birefringence (MB) measurements, intended to probe coupling of the field-induced nematic order (Q_{ij}) to additional order parameters, and dynamic light scattering (DLS) and flow viscosity experiments to uncover any unusual dynamical effects that may be associated with the I_1-I_2 transition. In the MB study, the field-induced birefringence (Δn) was measured, using the standard photoelastic modulation, lock-in-based optical signal recovery technique [18], as a function of temperature and field (H) at the National High Magnetic Field Laboratory (Cell 4). This technique detects Δn due to H-induced uniaxial optical anisotropy. For small magnitude of the uniaxial order parameter and H along the z axis, Δn is given by $\Delta n = \sqrt{\epsilon_{zz}} - \sqrt{\epsilon_{xx}} \approx (\Delta\epsilon/2\sqrt{\bar{\epsilon}})Q$, where $\epsilon_{ij} = \bar{\epsilon}\delta_{ij} + \Delta\epsilon Q_{ij}$ is the uniaxial dielectric tensor, $\bar{\epsilon}$ is the value of the dielectric constant in the fully isotropic phase, $\Delta\epsilon$ is the saturated dielectric constant anisotropy in the uniaxially ordered (nematic) phase, and $\Delta\epsilon \ll \bar{\epsilon}$. We have also used the expression for Q_{ij} in diagonal form, $Q_{xx} = Q_{yy} = -Q/3$ and $Q_{zz} = 2Q/3$. The standard LdG model of the isotropic-nematic transition in an applied H gives the orientational free energy as $F_Q = A_Q Q^2/2 - \Delta\chi H^2 Q$, where $A_Q = a_Q(T - T_Q^*)$ is the temperature-dependent leading Landau coefficient, T_Q^* is the supercooling limit for the isotropic phase, and $\Delta\chi$ is the saturated diamagnetic anisotropy in the nematic phase. Minimizing F_Q over Q, one therefore expects—and observes at all temperatures in the isotropic phase of typical rodlike calamitic liquid crystals [19,20] and for the largest available dc fields—a linear dependence of Δn on H^2, given by $\Delta n(H,T) = \Delta\epsilon\Delta\chi H^2/2\sqrt{\bar{\epsilon}}a_Q(T - T_Q^*)$.

Figure 3 shows representative data for Δn as a function of H^2, obtained on the bent-core compound ClPbis10BB for representative temperatures in the I_1 phase. In contrast to the conventional behavior in calamitics—and close to the I_1-I_2 transition detected by calorimetry—there is a significant deviation from linearity in H^2, characterized by a negative curvature. This curvature cannot be explained simply by introducing terms in F_Q that couple higher powers of H^2 to Q—e.g., by adding terms of the form QH^{2n} $(n>1)$ to the free energy expansion, which gives $\Delta n(H,T) = \Delta\epsilon[\Delta\chi H^2 + O(H^{2n})]/2\sqrt{\bar{\epsilon}}a_Q(T - T_Q^*)$. In this expression, all the coefficients of the powers of H^2 have the same T dependence, which implies that plots of $\Delta n(T,H)$ vs H^2 at different temperatures can be collapsed onto a single curve using field-independent factors of $T - T_Q^*$. Such a collapse does not apply to the data in Fig. 3, where the shape of the data vs H^2 clearly varies with T. One could also generate a nonlinear Δn vs H^2 behavior from field-dependent terms quadratic in Q

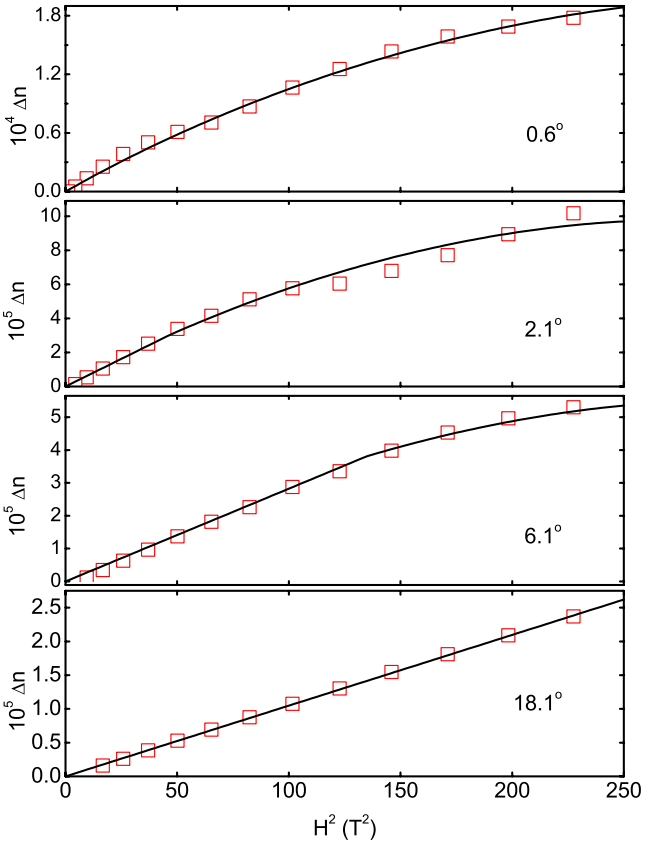

FIG. 3. (Color online) Induced refractive index anisotropy Δn as a function of applied field squared (H^2) on cooling in the higher-temperature isotropic (I_1) phase of ClPbis10BB. Specific temperature increments above the clearing point ($T-T_{cp}$, where T_{cp} =76.9 °C) are indicated in the figure. Note the deviation from the linear-in-H^2 dependence that develops closer to T_{cp}—a behavior that is uncharacteristic of calamitic liquid crystals. Solid lines represent fits to the model discussed in the text, which includes field-dependent coupling of nematic and tetrahedratic order parameters.

(e.g., Q^2H^{2n}), but, provided the corresponding Landau coefficients are not extremely large, we expect these terms to be negligible compared to the linear-in-Q coupling since, using parameters from Ref. [11], we estimate the maximum induced Q from our measurements of Δn is ~0.005.

We conducted light scattering studies of Q order parameter fluctuations (sensitive to the associated orientational viscosity (η_Q) and measurements of the flow, or Navier-Stokes, viscosity (η_{flow}) to search for a dynamical signature associated with the I_1-I_2 transition. In the light scattering experiments, the time correlation function of the depolarized scattered intensity, due to fluctuations δQ of the nematic order parameter, was recorded in the homodyne regime as a function of temperature above the clearing point at a fixed scattering wave number q=76 000 cm^{-1}. The intensity correlation data were well described by a single exponential relaxation. The relaxation rate (Γ) of the pretransitional nematic fluctuations for ClPbis10BB is shown in Fig. 4. With decreasing temperature, Γ shows a rather abrupt decrease in slope at a temperature ~3 °C above T_{cp}. As Fig. 5 reveals, this temperature region (above the I_1-I_2 transition associated with the higher-temperature specific heat peak in Fig. 1) also

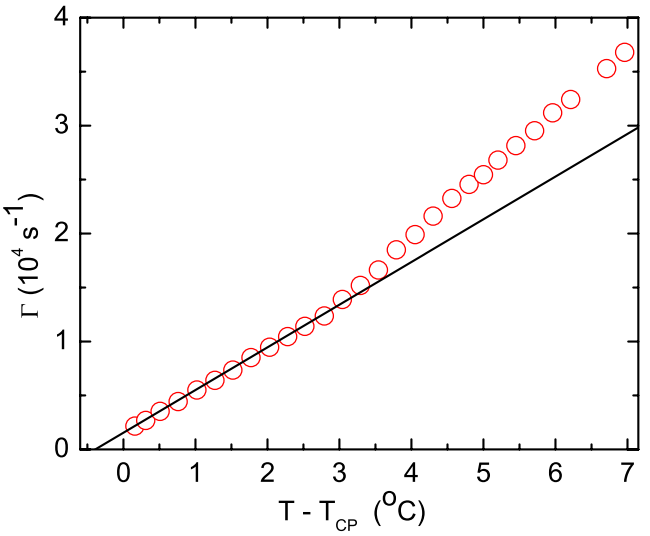

FIG. 4. (Color online) Relaxation rate Γ of fluctuations in Q as function of temperature above the clearing point in ClPbis10BB for fixed scattering vector q=76 000 cm^{-1}. Note the change in slope occurring for $T-T_{cp}$ just above 3 °C.

corresponds to a rapid increase in the order parameter viscosity η_Q. η_Q was calculated from the data for Γ, the relation $\Gamma=A_Q/\eta_Q=a_Q(T-T_Q^*)/\eta_Q$ (resulting from the usual Landau-Khalatnikov dynamical equation for the relaxation of Q), the value of T_Q^* obtained from the fit indicated by the solid line in Fig. 4, and the value of a_Q reported in Ref. [13].

The flow viscosity η_{flow} was measured using an electrorotation method, in which we recorded and analyzed the electric-field-induced rotation of the long axis of cylindrical glass rods ~5 μm diameter by ~30 μm length dispersed in the sample [21,22]. The effect is analogous to the field-induced rotation of a solid dielectric sphere in a liquid ("Quincke rotation") that occurs when the charge relaxation time for the sphere exceeds that of the liquid [23]. We utilized an ac electric field, with the frequency chosen at a

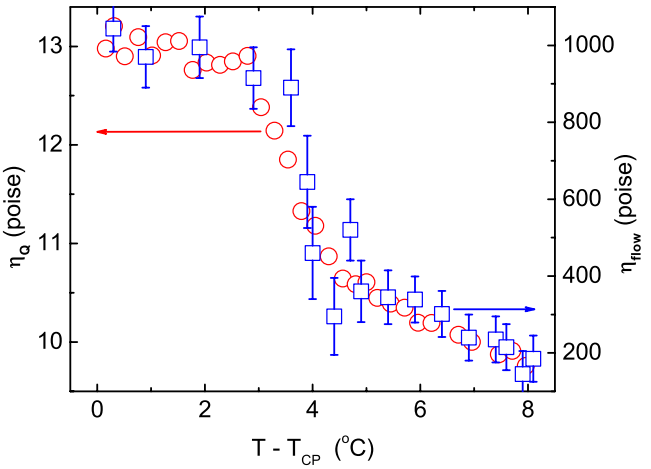

FIG. 5. (Color online) Orientational order parameter viscosity η_Q (circles) and flow viscosity η_{flow} (squares) in ClPbis10BB measured, respectively, by light scattering and by the electrorotation method described in the text, above the clearing point.

sufficiently high value to avoid any detectable reorientation of the liquid crystal optical axis. The angled ends of selected rods allows an accurate recording of the rotation by a digital camera, and subsequent analysis (taking into account the ac field and presented in detail elsewhere [22]) leads to a determination of η_{flow}. As Fig. 5 shows, η_{flow} exhibits a substantial increase on cooling at a temperature consistent with the rise in η_Q in the I_1 phase. It is interesting to note that η_{flow} increases by a factor of 5, whreas the increase in η_Q is more modest (a factor of 1.3).

Summarizing the experimental results presented so far, the heat capacity and mass density data above T_{cp} clearly reveal a transition in ClPbis10BB between optically isotropic phases occurring at a temperature $T_x \approx T_{\text{cp}}+0.4\ ^\circ\text{C}$, while the magnetic-field-induced birefringence (Δn) and both orientational and flow viscosities behave anomalously at temperatures above this transition (i.e., in the upper isotropic or I_1 phase). Thus any model to explain our results must both account for an additional isotropic phase, as well as for the unusual field dependence of Δn and sharp change in the viscosities observed above T_x.

One possibility is a nonchiral analog of the isotropic–blue-phase-III transition that occurs in certain chiral calamitic compounds [24,25]. A transition of similar symmetry could theoretically occur in a nonchiral bent-core compound if one considers specific achiral quadratic combinations of Q as potential secondary order parameters [26]. However, this theoretical possibility would imply a significant change in the temperature dependence of the intensity of light scattered by fluctuations δQ at the I_1-I_2 transition [26]—a change that is *not* observed in data we obtained for the inverse scattered intensity, which are presented in Fig. 7 and discussed further below. (Note that these data cover a temperature range both above and below T_x.)

An interesting alternative scenario for an optically isotropic–isotropic transition can be based on tetrahedratic order—i.e., orientational order characterized by a traceless symmetric third-rank tensor τ_{ijk} that does not confer optical anisotropy. Recent theoretical studies [11,12] have specifically argued that this model should be relevant to fluid phases of bent-core liquid crystals. Thus we suppose that the I_2 and I_1 phases are in fact the optically isotropic *tetrahedratic* (τ) phase and the fully isotropic (I) phase, respectively, and that the observed transition at the clearing point is between the τ phase and a *nematic-tetrahedratic* (N_τ) phase that possesses both tetrahedratic and ordinary nematic order.

As mentioned in the introduction, the model for the τ and N_τ structures is based on orientational ordering of complexes of bent-core molecules with tetrahedral symmetry. One would expect complexes or clusters to yield substantially higher viscosities relative to single molecules, due to their increased size and surface area, and possibly their potential for entanglement. In fact, the observed orientational and flow viscosities in Fig. 5 are dramatically higher—respectively, $\sim$10–100 and $\sim$1000 times—than in typical isotropic calamitics at comparable temperatures. The rise in the viscosities of ClPbis10BB that occurs on cooling at a temperature several degrees above both T_{cp} and T_x (Fig. 5) therefore suggests a pretransitional effect that could be associated with a change in cluster size or morphology (but no change in symmetry—i.e., the clusters remain orientationally disordered).

To explain the unusual pretransitional behavior in the field dependence of Δn (Fig. 3), we consider the following LdG free energy, which, in terms of order parameter amplitudes Q and τ, provides a "minimal" model to discuss induced nematic and tetrahedratic order in the vicinity of an I-τ transition and in the presence of a magnetic field H:

$$F = \frac{1}{2}A_Q Q^2 + \frac{1}{2}A_\tau \tau^2 + \frac{1}{4}c_\tau \tau^4 - \Delta\chi Q H^2 - w_{h1} H^2 Q \tau^2 - w_{h2} H^2 \tau^2. \tag{1}$$

Here $A_\tau = a_\tau (T - T_T^*)$, and T_τ^* represents the supercooling limit of the τ phase. The tetrahedratic order parameter amplitude τ represents the component of τ_{ijk} that orders at the I-τ transition—i.e., the component that is invariant under operations of the tetrahedral group T_d [11]. Since we are not at the moment interested in the lower-temperature transition to the nematic phase, we consider in Eq. (1) only the terms in Q that suffice to describe field-induced Q order. When $c_\tau > 0$, the zero-field I-τ transition is continuous at the mean field level, but it has been argued that thermal fluctuations, combined with specific properties of τ_{ijk}, drive the transition first order [27]. On the other hand, when $c_\tau < 0$, the transition is first order at the mean field level [and a sixth-order term would be needed in Eq. (1) to stabilize the tetrahedratic phase]. Thus, the data of Fig. 1 are consistent with a predicted first-order I-τ transition for general c_τ. The coefficient w_{h1} in Eq. (1) controls the lowest-order permissible field-dependent coupling $H^2 Q \tau^2$ between Q and τ. Due to parity and $\vec{H}$ being a pseudovector, terms of the form $HQ\tau$ are not allowed [12]. Moreover, *field-independent* terms of order $Q\tau^2$, which could in principle induce nematic order in a tetrahedratic phase, are not present due to the tracelessness of Q_{ij} and τ_{ijk}, and to a special property of τ_{ijk}—namely, $\Sigma_{i,j}\tau_{ijk}\tau_{ijl} \propto \delta_{kl}$ [12,27].

Minimizing F with respect to Q and inserting the result back into Eq. (1) yields

$$F_\tau = \frac{-\Delta\chi H^2}{2A_Q} + \left(\frac{A_\tau}{2} - \frac{w_{h1}\Delta\chi H^4}{A_Q} - w_{h2}H^2\right)\tau^2 + \frac{1}{2}\left(\frac{c_\tau}{2} - \frac{w_{h1}^2 H^4}{A_Q}\right)\tau^4. \tag{2}$$

If the coefficients of the second- and-fourth order terms in τ are both positive, the solution for minimum F is $\tau^2 = 0$. However, if the τ^2 coefficient is negative while that for τ^4 remains positive, F_τ is minimized for nonzero τ^2. Finally, if the coefficient of τ^4 is negative, a positive τ^6 term must be added to Eqs. (1) and (2) to stabilize the system. For simplicity, we shall assume that this is not the case—i.e., $H^2 < (\sqrt{A_Q c_\tau}/2)/|w_{h1}|$ for relevant fields and temperatures. (Since we consider $T > T_Q^*$, this also means that we assume $c_\tau > 0$.) Then vanishing of the coefficient of τ^2 in Eq. (2) implies critical fields given by

$$H_{c\pm}^2 = \frac{1}{2w_{h1}\Delta\chi}[-A_Q w_{h2} \pm \sqrt{(A_Q w_{h2})^2 + 2A_Q A_\tau w_{h1}\Delta\chi}]. \tag{3}$$

Since $\Delta\chi > 0$ for ClPbis10BB [13] and considering $A_Q, A_\tau > 0$ (i.e., $T > T_Q^*, T_\tau^*$), there are two real solutions for H_c when $w_{h1} < 0$ and $w_{h2} > 0$, one real solution when $w_{h1} > 0$, and no real solutions when $w_{h1} < 0$ and $w_{h2} < 0$. Combining these results with minimization of Eq. (1) over both Q and τ, plus the expression $\Delta n = \Delta\epsilon Q/2\sqrt{\bar{\epsilon}}$, we calculate the following.

For $w_{h1} < 0, w_{h2} < 0$,

$$\Delta n(H,T) = \frac{\Delta\epsilon}{2\sqrt{\bar{\epsilon}}}\frac{\Delta\chi H^2}{A_Q}. \tag{4}$$

For $w_{h1} > 0$,

$$\Delta n(H,T) = \begin{cases} \dfrac{\Delta\epsilon}{2\sqrt{\bar{\epsilon}}}\dfrac{\Delta\chi H^2}{A_Q}, & H^2 < H_{c+}^2, \\ \dfrac{\Delta\epsilon}{2\sqrt{\bar{\epsilon}}}\left(\dfrac{(c_\tau\Delta\chi - A_\tau w_{h1})H^2 + 2w_{h1}w_{h2}H^4}{c_\tau A_Q - 2w_{h1}^2 H^4}\right), & H^2 > H_{c+}^2. \end{cases} \tag{5}$$

For $w_{h1} < 0, w_{h2} > 0$,

$$\Delta n(H,T) = \begin{cases} \dfrac{\Delta\epsilon}{2\sqrt{\bar{\epsilon}}}\dfrac{\Delta\chi H^2}{A_Q}, & H^2 < H_{c-}^2 \text{ or } H^2 > H_{c+}^2, \\ \dfrac{\Delta\epsilon}{2\sqrt{\bar{\epsilon}}}\left(\dfrac{(c_\tau\Delta\chi + A_\tau|w_{h1}|)H^2 - 2|w_{h1}|w_{h2}H^4}{c_\tau A_Q - 2w_{h1}^2 H^4}\right), & H_{c-}^2 < H^2 < H_{c+}^2. \end{cases} \tag{6}$$

The expressions in Eq. (4) and Eqs. (5) and (6) (top) are the standard results one expects from field-induced Q in the absence of any induced τ order. As noted earlier, they clearly do not describe the curvature in the data in Fig. 3 for T close to T_{cp}. The consequences of the full results in Eq. (4)–(6) are best illustrated graphically. Figure 6 shows the shape of Δn vs H^2 predicted for different combinations of the signs of w_{h1} and w_{h2}, together with values of the various parameter combinations in Eqs. (4)–(6) that produce Δn in the experimentally observed range for $T - T_{cp} = 0.6°$. Comparing Figs. 3 and 6, it is clear that only the case $w_{h1} < 0$, $w_{h2} > 0$ matches the negative curvature of the actual data for $T - T_{cp} = 0.6°$ over the range of H^2 studied.

The solid lines in Fig. 3 are fits of the data to Eq. (6) that were performed over H and T simultaneously using one consistent set of fit parameters. Specifically, Δn in Eq. (6) was expressed in terms of the parameters $A_1 = \Delta\epsilon\Delta\chi/2\sqrt{\bar{\epsilon}}a_Q$, $A_2 = \Delta\epsilon a_\tau|w_{h1}|/2\sqrt{\epsilon}a_Q c_\tau$, $A_3 = \Delta\epsilon|w_{h1}|w_{h2}/\sqrt{\bar{\epsilon}}a_Q c_\tau$, $A_4 = 2w_{h1}^2/a_Q c_\tau$, T_Q^*, and T_τ^*. The value of A_1 was determined from a fit of the highest-temperature data in Fig. 3 to Eq. (4), while T_τ^* was fixed to the temperature of the higher heat capacity peak in Fig. 1—i.e., we took $T_\tau^* = T_x$. (In fact, we found that varying T_τ^* between T_Q^* and T_x did not substantially affect the quality of the fits—a result that may be partly explained by the fact that we obtained MB data only for $T > T_x$.) Thus, four temperature-independent parameters (A_2, A_3, A_4, T_Q^*) were used to fit the three lower-temperature data sets in Fig. 3. We note that the model provides a reasonable overall description of the data.

An important prediction of Eqs. (3) and (6) is that, while the critical fields $H_{c\pm}$ both shift to lower values as $T \to T_Q^*$ from above, for sufficiently low H we should still recover conventional behavior for Δn—namely, $\Delta n \sim H^2/(T - T_Q^*)$. Thus, taking the slope of the low-field data in Fig. 3, we should obtain the Cotton-Mouton coefficient, C_{CM}

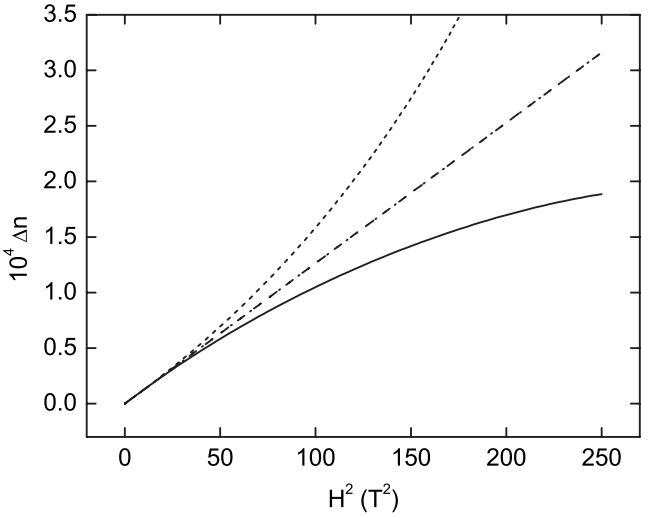

FIG. 6. Results from the model for Δn vs H^2 in Eqs. (4)–(6) plotted for representative values of the parameters in the model that place Δn in the range observed in the data in Fig. 3 for $T - T_{cp} = 0.6$ °C. Solid, short-dashed, long-dashed, and dotted lines represent the cases ($w_{h1} < 0$, $w_{h2} > 0$), ($w_{h1} > 0$, $w_{h2} > 0$), ($w_{h1} < 0$, $w_{h2} < 0$), and ($w_{h1} > 0$, $w_{h2} < 0$), respectively. (The plots for the last two cases overlap over the range of H^2 considered.)

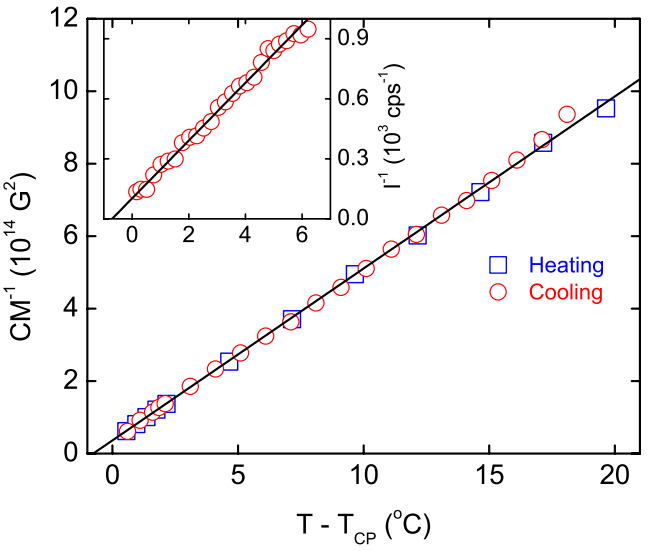

FIG. 7. (Color online) Inverse Cotton-Mouton coefficient C_{CM}^{-1} and inverse intensity I^{-1} of light scattered from nematic order parameter fluctuations, as functions of temperature T above the clearing point (T_{cp}) in ClPbis10BB. Solid lines represent linear fits in T.

$\equiv \lim_{H\to 0} \Delta n/H^2$, with the standard temperature dependence $C_{\mathrm{CM}}^{-1} \sim T - T_Q^*$. Figure 7 shows results for C_{CM}^{-1} vs T obtained from our full set of MB data for various temperatures above T_{cp}. We clearly observe the expected linear temperature dependence, and find $T_{\mathrm{cp}} - T_Q^* \approx 0.8$ °C, a value that is consistent with the fits presented in Fig. 3 but is several tenths of a degree higher than we found previously [13] from an MB study performed in fields below 1.3 T. The discrepancy in $T_{\mathrm{cp}} - T_Q^*$ is probably due to differences in experimental conditions: the samples used in the present and previous experiments came from two different batches of liquid crystal, and the fields used in our earlier work were much lower than those in the present study. For completeness, in Fig. 7 we also present data for the temperature dependence of the inverse intensity I^{-1} of light scattered from Q order parameter fluctuations. The zero-field Landau theory [Eq. (1) with $H=0$] combined with equipartition of energy predicts $I^{-1} \sim \langle \delta Q^2 \rangle^{-1} \sim T - T_Q^*$, which is confirmed by the data in Fig. 7 over the range of T where I could be reliably measured. Note that there is no predicted or observed effect of τ order on I^{-1}; this can be construed as a consequence of the particular property of τ_{ijk} (noted above) that rules out the lowest-order, field-independent, scalar contribution to the free energy one would normally construct by coupling Q_{ij} and τ_{ijk}.

To summarize, we have studied the bent-core liquid crystal ClPbis10BB at temperatures above the clearing point with various sensitive experimental techniques. Our measurements reveal a transition between two optically isotropic phases, which can be consistently explained by a model for tetrahedratic orientational order in bent-core liquid crystals. However, in spite of the range and consistency of experimental results, the evidence for such exotic order remains indirect and so cannot at present be viewed as conclusive. For the future, provided the effects of impurities can be tightly controlled, electric birefringence could prove a revealing experiment, since in this case symmetry permits a distinctive linear coupling ($EQ\tau$) in the free energy between the E field and the order parameters Q, τ [28]. Additionally, we are currently pursuing a number of other studies that could further reveal and characterize unconventional aspects of the isotropic and nematic phases of bent-core compounds. These include second-harmonic generation (the τ and N_τ phases should be noncentrosymmetric [11]), flow birefringence measurements, flow-induced electric current and its converse (as suggested in Ref. [12]), and small-angle x-ray scattering (to probe for evidence of nanoscale molecular clustering).

We would like to thank J. Kim, Q. Li, and K. Fodor-Csorba for assistance and provision of materials, H. Pleiner and T. Lubensky for helpful discussions, and W. Aldhizer, X. Wei, K. Sigdel, and B. Brandt for technical assistance. Work at Kent State was supported by NSF Grants No. DMR-0606160, No. DMS-0456221, and No. DMR-9988614, and at the National High Magnetic Field Laboratory by NSF cooperative agreement No. DMR-0084173, the state of Florida, and the DOE.

[1] T. Niori, T. Sekine, J. Watanabe, T. Furukawa, and H. Takezoe, J. Mater. Chem. **6**, 1231 (1996).
[2] D. R. Link, G. Natale, R. Shao, J. E. Maclennan, N. A. Clark, E. Korblova, and D. M. Walba, Science **278**, 1924 (1997).
[3] G. Pelzl, S. Diele, and W. Weissflog, Adv. Mater. (Weinheim, Ger.) **11**, 707 (1999).
[4] J. P. Bedel, J. C. Rouillon, J. P. Marcerou, M. Laguerre, H. T. Nguyen, and M. F. Achard, Liq. Cryst. **28**, 1285 (2001).
[5] H. R. Brand, P. E. Cladis, and H. Pleiner, Eur. Phys. J. B **6**, 347 (1998).
[6] L. A. Madsen, T. J. Dingemans, M. Nakata, and E. T. Samulski, Phys. Rev. Lett. **92**, 145505 (2004).
[7] B. R. Acharya, A. Primak, and S. Kumar, Phys. Rev. Lett. **92**, 145506 (2004).
[8] J. A. Olivares, S. Stojadinovic, T. J. Dingemans, S. Sprunt, and A. Jakli, Phys. Rev. E **68**, 041704 (2003).
[9] J. Harden, B. Mbanga, N. Eber, K. Fodor-Csorba, S. Sprunt, J. T. Gleeson, and A. Jakli, Phys. Rev. Lett. **97**, 157802 (2006).
[10] L. G. Fel, Phys. Rev. E **52**, 702 (1995).
[11] T. C. Lubensky and L. Radzihovsky, Phys. Rev. E **66**, 031704 (2002).
[12] H. R. Brand, H. Pleiner, and P. E. Cladis, Eur. Phys. J. E **7**, 163 (2002).
[13] D. Wiant, S. Stojadinovic, K. Neupane, S. Sharma, K. Fodor-Csorba, A. Jakli, J. T. Gleeson, and S. Sprunt, Phys. Rev. E **73**, 030703(R) (2006).
[14] V. Domenici, M. Geppi, C. A. Veracini, R. Blinc, A. Lebar, and B. Zalar, J. Phys. Chem. B **109**, 769 (2005).
[15] K. Fodor-Csorba, A. Vajda, G. Galli, A. Jakli, D. Demus, S. Holly, and E. Gacs-Baitz, Macromol. Chem. Phys. **203**, 1556

(2002).
[16] A. Roshi, G. S. Iannacchione, P. S. Clegg, and R. J. Birgeneau, Phys. Rev. E **69**, 031703 (2004).
[17] G. R. Van Hecke and J. Stecki, Phys. Rev. A **25**, 1123 (1982).
[18] T. Oakberg, Proc. SPIE **2873**, 17 (1996).
[19] P. H. Keyes and J. R. Shane, Phys. Rev. Lett. **42**, 722 (1979).
[20] C. Rosenblatt, Phys. Rev. A **25**, 1239 (1982).
[21] G. Liao, I. I. Smalyukh, J. R. Kelly, O. D. Lavrentovich, and A. Jakli, Phys. Rev. E **72**, 031704 (2005).
[22] E. Dorjgotov, K. Fodor-Csorba, J. T. Gleeson, S. Sprunt, and A. Jakli, Liq. Cryst. **35**, 149 (2008).
[23] T. B. Jones, IEEE Trans. Ind. Appl. **20**, 845 (1984).
[24] G. Voets and W. V. Dael, Liq. Cryst. **14**, 617 (1993).
[25] J. B. Becker and P. J. Collings, Mol. Cryst. Liq. Cryst. Sci. Technol., Sect. A **265**, 163 (1995).
[26] T. C. Lubensky and H. Stark, Phys. Rev. E **53**, 714 (1996).
[27] L. Radzihovsky and T. C. Lubensky, Europhys. Lett. **54**, 206 (2001).
[28] H. R. Brand, H. Pleiner, and P. E. Cladis, Physica A **351**, 189 (2005).